Science of the Total Environment 709 (2020) 136138

Contents lists available at ScienceDirect

Science of the Total Environment

journal homepage: www.elsevier.com/locate/scitotenv

Efficient biodegradation of highly crystallized polyethylene terephthalate through cell surface display of bacterial PETase

Zhuozhi Chen [a,1], Yanyan Wang [a,1], Yingying Cheng [a], Xue Wang [a], Shanwei Tong [a], Haitao Yang [a], Zefang Wang [a,b,*]

[a] School of Life Sciences, Tianjin Key Laboratory of Function and Application of Biological Macromolecular Structures, College of Precision Instrument and Opto-electronics Engineering, Tianjin University, Tianjin, 300072, China
[b] Tianjin International Joint Academy of Biotechnology and Medicine, Tianjin 300457, China

HIGHLIGHTS

- Yeast cell surface display bacterial PETase can degrade different commercial highly crystallized PET.
- The turnover rate of the PETase-displaying yeast whole-cell biocatalyst increased about 36-fold.
- The whole-cell biocatalyst system is reusable and robust.

GRAPHICAL ABSTRACT

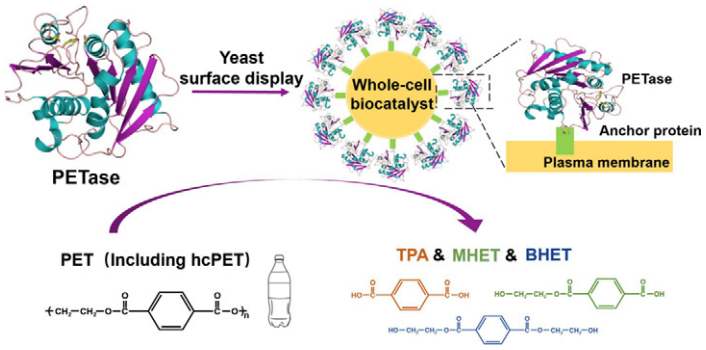

ARTICLE INFO

Article history:
Received 29 September 2019
Received in revised form 13 December 2019
Accepted 14 December 2019
Available online 16 December 2019

Editor: Jay Gan

Keywords:
Biodegradation
Polyethylene terephthalate
PETase
Yeast cell surface display
Whole-cell biocatalyst

ABSTRACT

Polyethylene terephthalate (PET) is one of the most widely used plastics in the world. Accumulation of the discarded PET in the environment is creating a global environmental problem. Recently, a bacterial enzyme named PETase was found to have the novel ability to degrade the highly crystallized PET. However, the enzymatic activity of native PETase is still low limiting its possible use in recycling of PET. In this study, we developed a whole-cell biocatalyst by displaying PETase on the surface of yeast (*Pichia pastoris*) cell to improve its degradation efficiency. Our data shows that PETase could be functionally displayed on the yeast cell with enhanced pH and thermal stability. The turnover rate of the PETase-displaying yeast whole-cell biocatalyst towards highly crystallized PET dramatically increased about 36-fold compared with that of purified PETase. Furthermore, the whole-cell biocatalyst showed stable turnover rate after seven repeated use and under some chemical/solvent conditions, and its ability to degrade different commercial highly crystallized PET bottles. Our results reveal that PETase-displaying whole-cell biocatalyst affords a promising route for efficient biological recycling of PET.

* Corresponding author at: School of Life Sciences, College of Precision Instrument and Opto-electronics Engineering, Key Laboratory of Systems Bioengineering (Ministry of Education), Tianjin University, Tianjin 300072, China.
E-mail addresses: zhuozhichen@tju.edu.cn (Z. Chen), yanyanwang@tju.edu.cn (Y. Wang), 2017226005@tju.edu.cn (Y. Cheng), tongshanwei@tju.edu.cn (S. Tong), yanght@tju.edu.cn (H. Yang), zefangwang@tju.edu.cn (Z. Wang).
[1] These authors contributed equally to this work.

https://doi.org/10.1016/j.scitotenv.2019.136138
0048-9697/

1. Introduction

Polyethylene terephthalate (PET) is the most widely used synthetic polyester over the world due to its excellent combination of mechanical, chemical and thermal properties. In 2015, the global PET production reached approximately 27.8 million tons for dominant manufacturing of packaging materials and beverage bottles (https://www.plasticsinsight.com/global-pet-resin-production-capacity/, 2016). The strong demand of PET has brought a global problem that is how to efficiently deal with the post-consumer PET or the PET waste which can accumulate and stay in the environment for hundreds of years due to its durability property. Multiple studies have shown that more than 690 species of marine organisms have been found to accumulate the PET debris and microplastics in their bodies, which means that PET has spread extensively from human food intake (Cressey, 2016; Zhang et al., 2017; Hahladakis et al., 2018).

Currently, recycling of PET has been considered as the best approach to resolve the PET waste problem (Sardon & Dove, 2018; Benavides et al., 2018). Several strategies have been developed to recover used PET including chemical, physical and biological treatments. Among them, physical recycling is a relatively simple and inexpensive method by direct converting PET into new end products through physical treatments like cutting, heating, extrusion and so on (Lin & Yang, 2007). However, this process refers to the deterioration of the product's properties in each cycle. In contrast, chemical recycling involves chemically converting used PET to monomers or partially depolymerized oligomers without significant degradation or waste (Lin & Yang, 2007). Although this method is a typical closed-loop recycling process, it is criticized because of generating secondary environmental pollution problem and high-energy consumption.

In recent years, biological recycling has attracted lots of attention since it can provide a “green route” for recycling PET with several advantages, such as easy operation, environmentally friendly, energy saving and minimizing waste (Zhang et al., 2017; Taniguchi et al., 2019; Shoda et al., 2016). It is derived from the discovery of microorganisms in the PET accumulation environment. The microorganism firstly secretes extracellular enzymes which depolymerize PET outside the cells generating water-soluble intermediates. Then those small molecules can be transported into the microorganisms for further digestion and metabolism (Shah et al., 2008; Guebitz & Cavaco-Paulo, 2008). Therefore, it is deduced that the efficiency of extracellular degradation enzymes is a key step affecting the outcome of the biological recycling of PET. So far, a number of PET degradation enzymes have been found including esterases, lipases, and cutinases (Doris et al., 2013; Groß et al., 2017; Joo et al., 2018). Those enzymes indeed can depolymerize the amorphous or low crystallinity PET to some extent. However, they lack the ability to cleave the high crystallinity PET which is used to produce beverage bottle routinely (Kawai et al., 2019).

Things really turned around in 2016 when a research group from Keio University identified a novel PET-hydrolyzing enzyme named PETase from a bacterium, *Ideonella sakaiensis* 201-F6 (Yoshida et al., 2016). This enzyme contains several distinct properties over other well-known PET-hydrolyzing enzymes. Other than high substrate specificity for PET and preserving enzymatic activity at low temperatures like 30-degree, the most valuable character of PETase is that it shows enzymatic activity towards PET with high crystallinity. Those unique properties together make PETase as a promising candidate for practical use in the field of PET recycling. Most recently, pioneering studies have been taken to determine the crystal structure and construct enzyme mutants for illuminate the molecular mechanism of PET degradation and improve its enzyme activity respectively. However, the enzymatic activity of PETase towards high-crystallized PET is still low limiting its possible use in large scale recycling of PET (Fecker et al., 2018; Liu et al., 2018).

It is quite clear that more studies need to be done to further improve the performance of PETase accelerating its industrial application. Therefore, we constructed several engineered yeast cells displaying PETase to improve its degradation efficiency of high-crystallized PET in our study(Chen et al., 2016; Bornscheuer et al., 2012; Simon et al., 2009; Yin et al., 2016; Liu et al., 2019; Yang et al., 2017). Different methods were employed to characterize the efficiency of the surface display system. Our results showed that PETase could be functionally displayed on the yeast cell, and the turnover rate of displayed PETase increased about 36.3-fold compared with that of native PETase. Furthermore, the whole-cell biocatalyst could be reused for seven times without obvious activity loss. This work provided valuable information on how to perform the whole-cell biocatalyst of PET using PETase and may lead to a feasible path towards the industrial application of PETase.

2. Materials and methods

2.1. Strains and culture conditions

The microbial strains and plasmids used in this study are listed in Supporting Information (SI) Table S1. *Pichia pastoris* (*P. pastoris*) strain GS115 and *Escherichia. Coli* (*E. coli*) DH5α were stored in our laboratory. *E. coli* DH5α was used in pPIC9 plasmid construction and was incubated at 37 °C in LB medium (1% *w/v* tryptone, 0.5% w/v yeast extract, and 1% w/v NaCl) supplemented with 100 μg/mL ampicillin. *P. pastoris* GS115 was cultured at 30 °C in the following media: YPD (1% w/v yeast extract, 2% w/v peptone, and 2% w/v glucose) for sub-cultivation, BMGY (1% w/v yeast extract, 2% w/v peptone, 100 mM potassium phosphate pH 6.0, 1.34% w/v yeast nitrogen base, and 1% *v*/v glycerol) for cell growth, and BMMY (1% w/v yeast extract, 2% w/v peptone, 100 mM potassium phosphate pH 6.0, 1.34% w/v yeast nitrogen base, and 1% v/v methanol) for recombinant protein production.

2.2. Amplification of target genes

The codon-optimized PETase gene sequence (**Sequence S1**) was synthesized by BGI Group (China). All primers used for plasmid construction were synthesized by GENEWIZ (China) are listed in SI Table S2. The *gcw21* (NCBI Reference Sequence: XM_002491407), *gcw51* (NCBI Reference Sequence: XP_002493782), and *gcw61* (NCBI Reference Sequence: XP_002494322) gene were amplified by polymerase chain reaction (PCR) from the genomic DNA of *P. pastoris* GS115 using primers 21/51/61-F and 21/51/61-R, containing an overlap area at the 5′-terminus and an *EcoR I* site at the 3′-terminus. The PETase gene was amplified by PCR with primers P—F and P-R, containing an *Xho I* site and a flag tag at the 5′-terminus and an overlap area at the 3′-terminus. All the PCR products were gel-purified, and then through overlap PCR, the fusion fragments PETase-GCW21/51/61 were successfully built.

2.3. Vector construction and yeast transformation

The fusion fragments were digested with corresponding restriction enzymes. The digested fragments PETase-GCW21/51/61, along with plasmid pPIC9 digested with *Xho I* and *EcoR I*, were ligated at 22 °C for 30 min, transformed into *E. coli* DH5α, and screened for positive clones. The resulting recombinant plasmids from positive clones named pPIC9-PETase-GCW21/51/61 were purified and verified by restriction enzyme digestion and sequencing. To display PETase on the cell surface, the new recombinant plasmids were linearized with *Stu I* and then transformed into *P. pastoris* GS115 by electroporation. Finally, the genome of the positive transformants selected from YPD plates containing 100 μg/mL ampicillin as the selective marker was used as a template, and PCR was carried out using the target gene primers and AOX primers respectively to screen out the true positive transformants.

2.4. Enzymatic activity assay of GS115/PETase-GCW21/51/61

GS115/PETase-GCW21/51/61 cells (4×10^7/mL, induced for 48 h) incubated with PET film (Good Fellow, crystallinity 45%, thickness 0.175 mm, diameter 6 mm) in buffer containing 50 mM glycine-NaOH (pH 9.0) for 18 h at 30 °C. Then the enzymatic activity of surfaced displayed PETase was determined by calculating the "turnover rate" of surfaced displayed PETase at each experiment. The turnover rated was calculating by normalizing the amount (moles) of mono (2-hydroxyethyl) terephthalic acid (MHET) produced in each experiment to the amount (moles) of PETase present in each experiment, then the resultant ratio is further divided to enzymatic degradation time (18×3600 s). The amounts of MHET and surface displayed PETase were calculated according to the detailed methods in the supplementary information (SI). All the following enzymatic activities of displayed or native PETase were determined in the same way.

2.5. Growth curve measurement of P. pastoris GS115 displaying PETase

The transformant of GS115/PETase-GCW51 was inoculated into BMGY medium at 30 °C to an optical density 600 (OD_{600}) of 2 to 6. The culture was centrifuged at 3500 ×*g* for 5 min and resuspended in BMMY medium to $OD_{600} = 1$. Methanol was added every 24 h to a final concentration of 0.5% (*v*/v) for inducing the expression of the fusion protein. *P. pastoris* GS115 was used as a negative control. OD_{600} was measured every 24 h from 0 h to 96 h, and the growth curve was drawn.

2.6. Optimization of the surface display system

To optimize induction time, GS115/PETase-GCW51 was induced for 0 h, 24 h, 48 h, 72 h, and 96 h for enzyme activity assay. To optimize pH, the reactions were conducted in 50 mM NaH_2PO4-NaOH (pH 5.0), 50 mM Na_2HPO4-HCl (pH 6.0–8.0), or 50 mM glycine-NaOH (pH 9.0–10). To optimize temperature, the reactions were conducted at 20 °C, 30 °C, 40 °C, and 50 °C, respectively.

2.7. Degradation of BHET and pNP-aliphatic esters with the whole-cell biocatalyst

The cells (4×10^7/mL) and purified PETase (0.303 μg/mL) were respectively incubated with 0.9 mM BHET (Sigma-Aldrich) in 40 mM Na_2HPO4-HCl (pH 7.0), 80 mM NaCl, and 20% (*v*/v) DMSO for 18 h at 30 °C, and were respectively incubated with 1 mM para-nitrophenol (*p*NP)-acetate, *p*NP-butyrate, and *p*NP-octanoate (Sigma-Aldrich) in 45 mM Na_2HPO4-HCl (pH 7.0), 90 mM NaCl, and 10% (v/v) DMSO for 5 min at 30 °C. The production of *p*NP was monitored at a wavelength of 415 nm.

2.8. Reusability and stability assays of the whole-cell biocatalyst

For the thermostability of yeast, the residual yeast activity was measured after incubation at 30 °C for 1–7 days in 50 mM glycine-NaOH buffer (pH 9.0). For the recycling of yeast, the yeast is recycled after centrifugation at 3500 ×*g*, 5 min. For the chemical/solvent conditions stability of yeast, the residual yeast activity was measured after incubation in 50 mM glycine-NaOH (pH 9.0), supplemented with methanol (final concentration, 10% v/v), ethanol (final concentration, 10% v/v), and Triton X-100 (final concentration, 0.1% v/v) for 18 h at 30 °C. Then the PET reaction was started after washing 3 times with 50 mM glycine-NaOH (pH 9.0) at 3500 ×*g*, 5 min.

2.9. Degradation of commercial PET bottles with the whole-cell biocatalyst

GS115/PETase-GCW51 cells (total cell number is 1.44×10^9) were respectively incubated with 6 mm diameter hcPET cut out from different commercial PET bottles (brands: Coca-cola, Nestlé, and Pepsi-cola) in 50 mM glycine-NaOH buffer (pH 9.0) for 18 h at 30 °C. The production of MHET was quantified by HPLC.

3. Results and discussion

3.1. PETase was functionally displayed on the yeast cell surface

PETase has several unique structural properties compared to other PET hydrolases. Fig. 1A shows the cleft of active-site in PETase seems to be much broader than those of the other PET hydrolases. Fig. 1B shows the substrate model binding site of PETase. It is clear that PETase forms a long, shallow L-shaped cleft on its protein surface. This substrate binding cleft is mainly hydrophobic and is crucial for the enzyme activity of PETase (Austin et al., 2018). These peculiar structural features may explain why PETase can accommodate and degrade highly crystallized substrate PET efficiently. Therefore, a flexible linker (GGGGSGGGGS) was used and linked the C terminal of PETase and N terminal of anchor proteins (Fig. S1) to increase chances for fully exposing the active and substrate binding sites of PETase when we constructed the surface display system (Wu et al., 2018; Xiaoying et al., 2013; He et al., 2016). Fig. 1C shows the schematic diagram of PET degradation process of the surface-displayed PETase.

It is well known that anchoring proteins affect the outcome of the surface display system (He et al., 2016; Annie & Dane, 2007). Among them, glycosylphosphatidylinositol (GPI)-anchored proteins have been applied for displaying various proteins on the yeast cell wall in the pharmacological and food fields (Lebreton et al., 2018; Lee et al., 2011; Mann et al., 2015). In our study, we selected three different endogenous GPI-modified cell wall proteins (GCW21, GCW51 and GCW61) from the host strain GS115 for use as anchor proteins to display PETase. Fig. 1D shows the western blot result of total protein from the corresponding recombinant GS115 strains with different anchor proteins. Three independent positive bands confirmed that PETase-GCW21, PETase-GCW51, and PETase-GCW61 were successfully expressed in the recombinant host strain, but we didn't know whether those three fusion proteins were delivered to the cell wall at this stage. Therefore, we performed immunofluorescence staining to verify PETase was successfully displayed on the cell wall of the host strain. As shown in Fig. 1E, there was no fluorescent signal observed inside the cells. In contrast, the strong immunofluorescent staining of yeast cell surface confirmed the correct surface display of PETase on the yeast cells, no matter what anchor protein was used. For the control, the fluorescence of non-induced cells with the same anchor protein was undetectable (Fig. S2). These results demonstrated PETase was successfully displayed on the yeast cell surface by using those three GPI proteins. Moreover, we found that the display efficiency was approximately 100% by counting the fluorescence-positive cells in our study for each anchor protein (Fig. S3). Considering the normal display efficiency of yeast was about 85% (Goyal et al., 2011), the relative high display efficiency in our study laid a good foundation of later application.

To further confirm the surface displayed PETase was biologically functional, we measured the enzyme activity of PETase displayed on the yeast cell. Yoshida S et al. reported that PETase dominantly converted PET to MHET, together with minor amounts of terephthalic acid (TPA) and bis(2-hydroxyethyl)-TPA (BHET) (Yoshida et al., 2016). Fig. 1F shows the measurement of the degradation products of PET degraded by surface displayed PETase with different anchor proteins using high-performance liquid chromatography (HPLC) system. The major product released by the displayed enzyme was MHET, trace amounts of TPA and BHET were detected at the same time. This result was consistent with that of native PETase suggesting the PETase was successfully displayed on the yeast cell surface with biological activity. Fig. 1G shows the quantitative analysis of HPLC results from Fig. 1F, it was clear that PETase with GCW51 anchor protein had the highest enzymatic activity, since its turnover rate against PET was higher than those

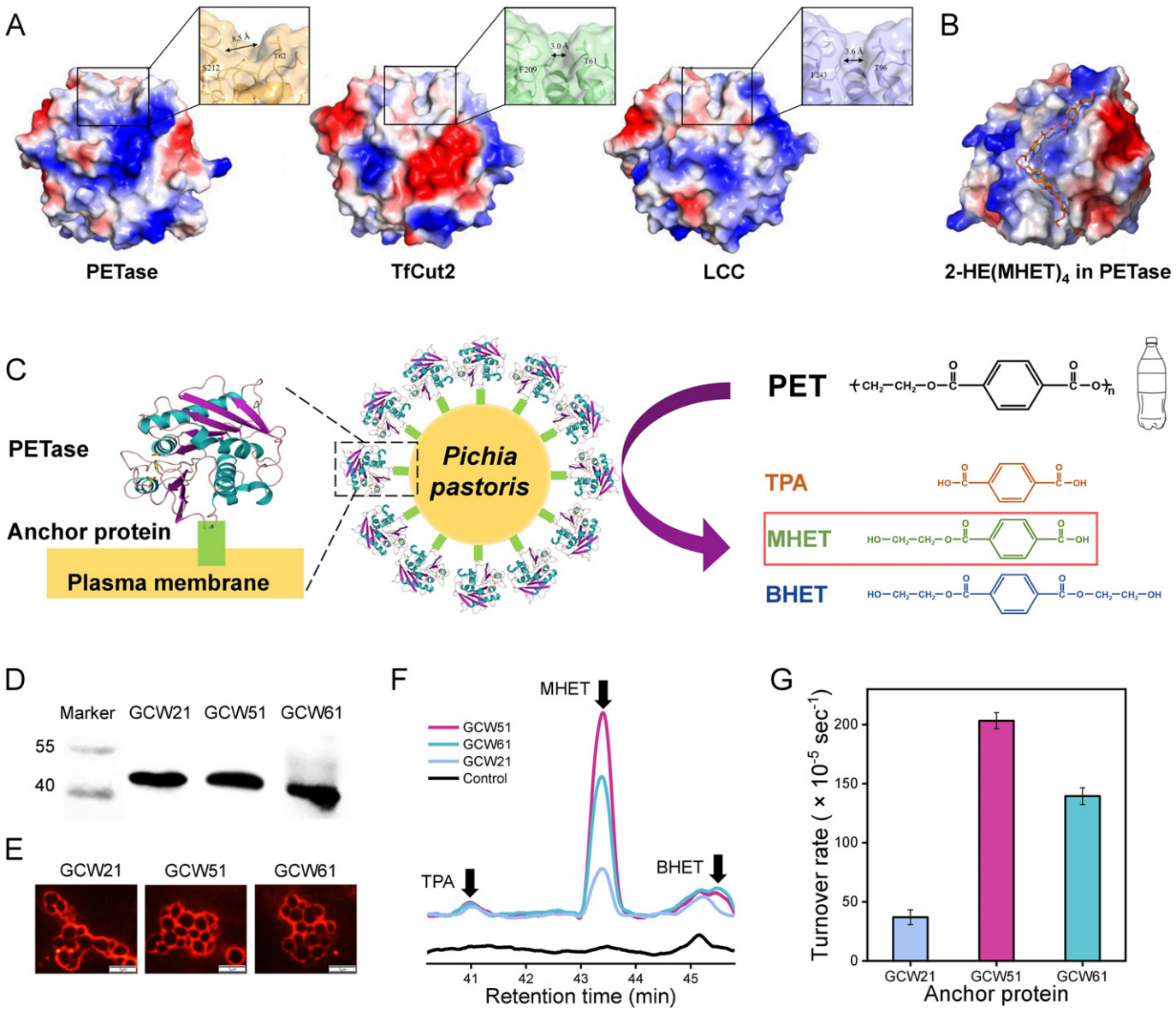

Fig. 1. (A) Comparison of substrate binding pocket of PETase, TfCut2, and LCC. The partially enlarged view shows the widest point of the substrate pocket. (B) Substrate binding site of PETase, 2-HE(MHET)$_4$, a four-MHET molecule was used to mimic PET. (C) PETase surface-displayed on the yeast (*P. pastoris*) host cell. (D) Western blot analysis of PETase-GCW21/51/61. (E) Immunofluorescence staining of PETase-GCW21/51/61. (F) HPLC analysis of the products released from the PET film which was degraded by PETase-GCW21/51/61 displayed on the yeast cell. (G) Quantitative analysis of HPLC results, turnover rate was used to evaluate the enzymatic activity of PETase-GCW21/51/61 displaying cells.

of PETase with GCW21 and GCW61 anchor proteins. This result confirmed that the selection of anchor protein was crucial for the surface display system (Annie & Dane, 2007). In the future, more anchor proteins should be tested to determine the best anchor protein for the display of PETase. Nevertheless, we used GCW51 as the anchor protein in the following studies.

3.2. Induction time-dependent enzyme activity of surface displayed PETase

After the successful surface display of PETase, the yeast cell will be used as a whole-cell biocatalyst for PET degradation. Therefore, the production of this whole-cell biocatalyst is important for the coming practical application. Regarding the yeast cell, the expression of foreign proteins may stress its growth and finally affect the cell density after the culture. Therefore, we measured the growth curve of wild-type the recombinant GS115 strain to determine whether the displayed PETase imposed a growing burden on the yeast cell. As shown in Fig. 2A, although the growth rate of the recombinant strain was slightly faster at some time points, the overall growth rates were quite similar for both wild-type and the recombinant GS115 strain indicating that surface display of the PETase brought a negligible burden on the growth of host strain. In the culture process of the recombinant GS115 strain, the inducer methanol was added into the medium to induce the surface display of PETase. Several studies pointed out the induction time had a significant influence on the biological activity of displayed enzymes (Wu et al., 2017; Xihong et al., 2015). The optimal induction time varied according to the target protein, vector and the host strain used in the surface display system. Therefore, the optimal induction time for surface display of PETase was examined in our study. Fig. 2B shows the total protein amount of PETase increased with the increasing of induction time. Most of the increase took place at 48 h, but this process seemed to continue at 72 and 96 h (Fig. S4). The immunofluorescent staining of surface-displayed PETase obtained the similar result (Fig. 2C). All the results together indicated that induction time posed an important influence on the expression levels of PETase on the yeast surface. To further investigate the relationship between surface-displayed PETase

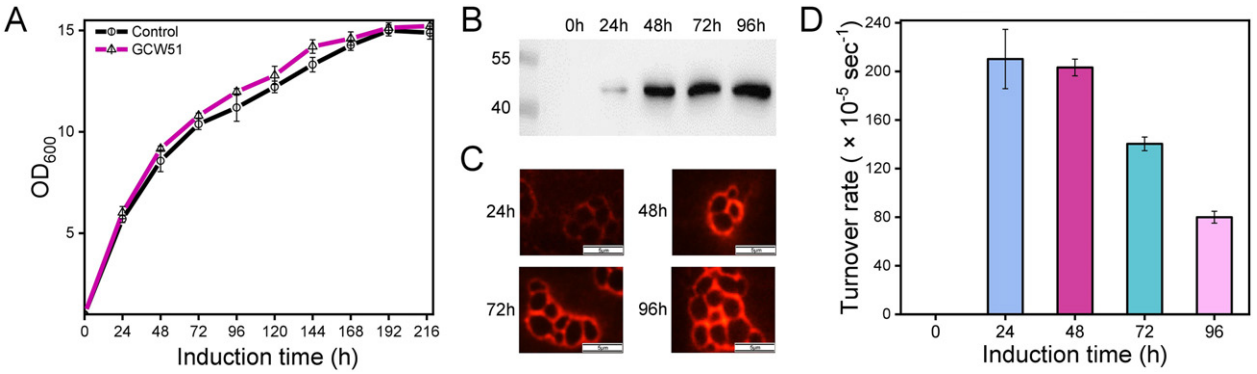

Fig. 2. (A) Growth curve of wild type *P. pastoris* GS115 and recombinant *P. pastoris* GS115/PETase-GCW51. (B) Western blot analysis of the expression of PETase-GCW51 under the induction time of 0, 24, 48, 72, and 96 h. (C) Immunofluorescence staining of the expression of PETase-GCW51 under the induction time of 24, 48, 72, and 96 h. (D) Turnover rates of *P. pastoris* GS115/PETase-GCW51 under the induction time of 0, 24, 48, 72, and 96 h.

expression and the enzyme activity, we examined the enzymatic activity of the yeast cells displaying PETase. Fig. 2D shows the changes of turnover rate of surface displayed PETase at different induction times. The turnover rates were almost identical at 24 and 48-h of induction. However, a sharp decline of the turnover rate was happened after 48 h of induction. In our degradation system, it was clear that the only variable was the amount of PETase displayed on the yeast cell surface, and this variable (displayed PETase) increased with the increasing of induction time. Since most of the PETase increase took place at 48 h, we proposed that the amount of displayed PETase reached a critical point at this particular induction time when displayed PETase could maintain high turnover rate (or enzymatic activity). A continuous increase of the number of displayed PETase molecules (at 72 and 96 h) would be denied the access to surface of the substrate PET, and these increased hindered active sites might result in the rapid drop overall turnover rate after 48 h of induction. Therefore, we chose 48 h as the induction time for producing the whole-cell biocatalyst in the following studies. The relatively shorter induction time means we can lower the cost in the production of the whole-cell biocatalyst for future industrial applications (Xihong et al., 2015).

3.3. Optimization of the surface display system

To further improve the performance of the surface display system, we investigated the effects of main factors on its catalytic ability, including pH, temperature and cell number (Chen et al., 2016; Wu et al., 2008; Paul et al., 2005; Liu et al., 2010). Fig. 3A shows the effect of pH on the turnover rate of the whole-cell biocatalyst. The turnover rate increased gradually in the range of pH 5–9 and reached the maximum at pH 9. While it reduced when pH value was above 9. Native PETase had a similar change pattern of enzyme activity like the whole-cell biocatalyst (Yoshida et al., 2016). However, the turnover rate of the whole-cell biocatalyst was higher than that of native PETase protein at each tested pH. This result indicated the pH stability of PETase was increased obviously at some conditions after it was displayed on the yeast cell. Considering many industrial processes may not be carried out at optimal pH value, the higher tolerance for pH at different levels would make displayed PETase more suitable for practical degradation of PET (Liu et al., 2010).

Next, we investigated how temperature affected the turnover rate of the whole-cell biocatalyst. As shown in Fig. 3B, the turnover rate of displayed PETase was remarkably increased at all tested temperatures when compared with the native PETase, but they both obtained the highest activity at 40 °C. These results revealed that displayed PETase was more active against PET at low temperatures. In a very recent review, Kawai et al. pointed that the heat-labile property of PETase might compromise its degradation efficiency because enzymatic degradation of PET was controlled by its chain mobility which was promoted at higher temperatures (Kawai et al., 2019). From this point of view, we could further optimize our surface display system to increase the thermal tolerance of the displayed PETase in the future. Finally, we determined the optimal number of the host cell with displayed PETase on its surface. To facilitate comparison, we normalized the cell numbers into protein concentration according to the strategy in the Figs. S5 and S6. Fig. 3C shows the effect of protein concentration on the turnover rate of the whole-cell biocatalyst. The turnover rates for the surface-displayed PETase were almost identical when the protein concentration was lower than 11 nM. With the increase of protein concentration (above 11 nM), the turnover rate dropped quickly. Regarding the native PETase, high turnover rates were observed when the protein concentration was lower than 370 nM, and the turnover rate was decreased rapidly at other higher protein concentrations. This result was very consistent with the result reported by Yoshida and his colleagues (Yoshida et al., 2016). All the above results indicated the protein concentration had a great influence on the turnover rate of PETase. In other words, overcrowding effects from the increase of protein concentration might happen and play an important role in hindering the reactivity of PETase molecules that did have access to the PET surface in both cases. When compared the maximum turnover rate of displayed PETase and native one, we found it was dramatically increased (about 36.3-fold) after it was displayed on the yeast cell (Fig. 3D).

3.4. The enzymatic activity of PETase was enhanced for different substrates

To further prove the enzymatic activity of surface-displayed PETase was increased, we tested its degradation capacity for different substrates including BHET and three *p*NP-aliphatic esters. As shown in Fig. 4A, the surface-displayed PETase could degrade BHET like native PETase. Furthermore, the turnover rate of surface-displayed PETase was obviously increased when compared with that of the native one. Several studies previously used BHET as the substrate to study the hydrolytic activities of native PETase and its mutants by monitoring the amount of produced MHET with HPLC analysis (Liu et al., 2018; Han et al., 2017). They found that enzymatic activity of native PETase could be improved up to 20% by mutating the Arg280 residue which might involve in the substrate binding. Regarding *p*NP-aliphatic esters, they were used initially to prove the substrate specificity of PETase against PET (Joo et al., 2018). It was found that PETase exhibits lower turnover rate on *p*NP-aliphatic esters which were the preferred substrates for lipases and cutinases (Yoshida et al., 2016). Fig. 4B shows clearly the turnover rate of surface-displayed PETase was greatly strengthened, no matter what *p*NP-aliphatic ester was used as the substrate. Like the native PETase, displayed PETase showed different turnover rates according to the carbon chain length of *p*NP-aliphatic ester. Maximal turnover rate was achieved when *p*NP-acetate (C2) was the degradation substrate, and the turnover rate decreased rapidly with the increased carbon chain length. Taken all of the above results together, we

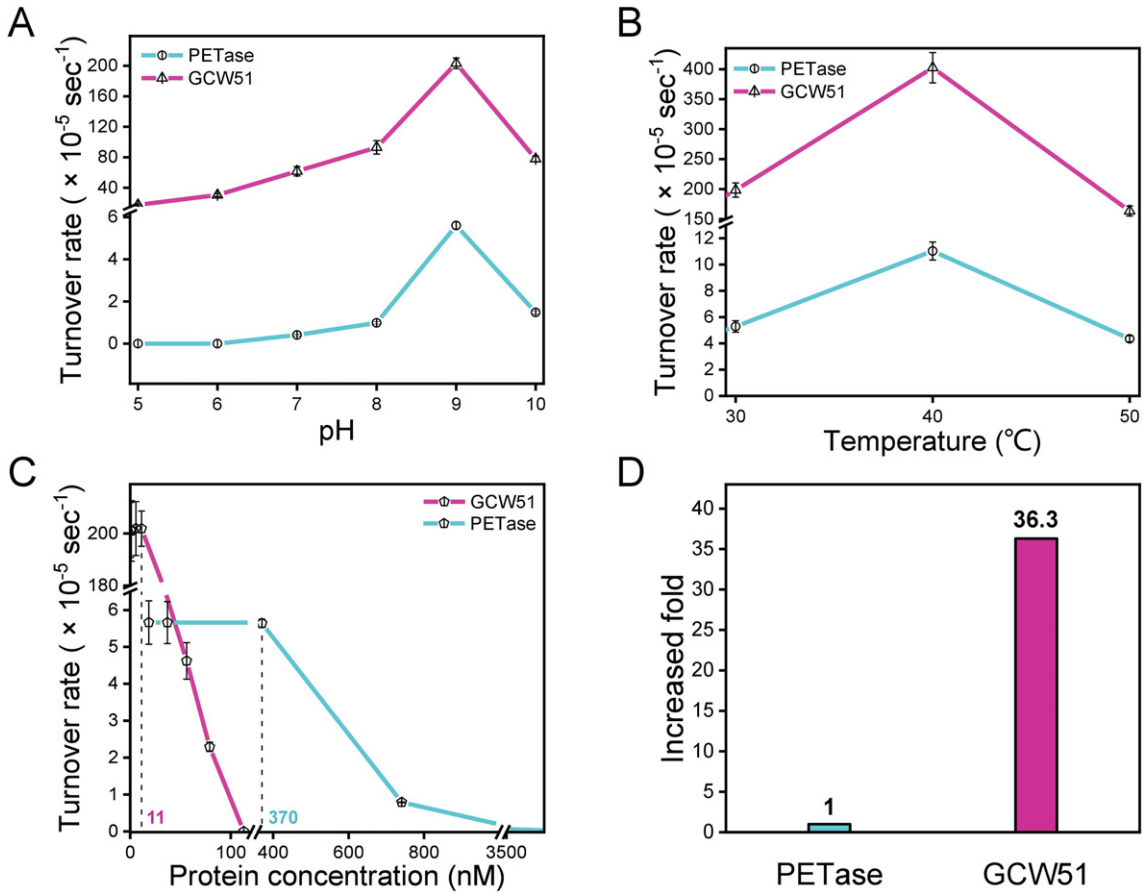

Fig. 3. (A) Effect of pH (B) temperature and (C) protein concentration on PET hydrolysis. (D) Comparison of turnover rate of native and surface-displayed PETase at the optimal condition.

concluded that the enzymatic activity of PETase was indeed enhanced with different scales for different substrates. This finding is very encouraging for developing the whole-cell biocatalyst system.

3.5. The whole-cell biocatalyst system is robust and efficient

When we apply the whole-cell biocatalyst to degrade PET, one primary consideration is how long the reaction system can be sustained at the operating temperature (Cooney, 1983; Zhang et al., 2016). Fig. 5A shows the thermostability curves of the whole-cell biocatalyst and purified PETase at 30 °C. For the whole-cell biocatalyst, the turnover rate of PET has almost no change with seven days. In contrast, the turnover rate of purified PETase decreased rapidly with the increase in incubation time. These results indicated that the thermostability of the whole-cell biocatalyst was increased compared with that of native PETase at 30 °C. Another consideration when we use the whole-cell biocatalyst is if this system can be reused to reduce the operation cost in degradation processes (Zhu & Wei, 2019; Tanaka & Kondo, 2015).

Technologically, recycle of the yeast cell is rather simple and can be easily achieved by centrifugation. However, the uncertain of the

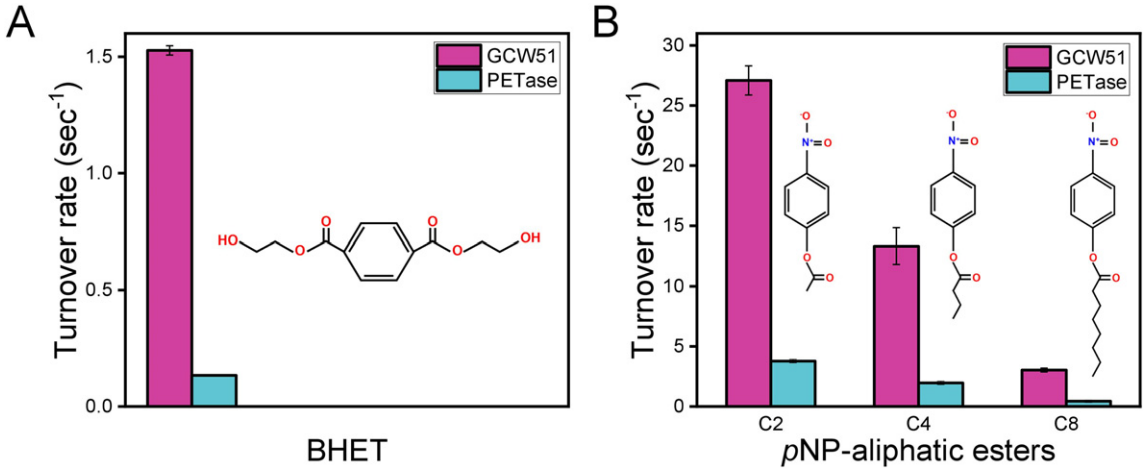

Fig. 4. (A) Turnover rates of GS115/PETase-GCW51 cells and purified PETase using BHET as a substrate. (B) Turnover rates of GS115/PETase-GCW51 cells and purified PETase using *p*NP-aliphatic esters as substrates. C2 is *p*NP-acetate. C4 is *p*NP-butyrate. C8 is *p*NP-caprylate.

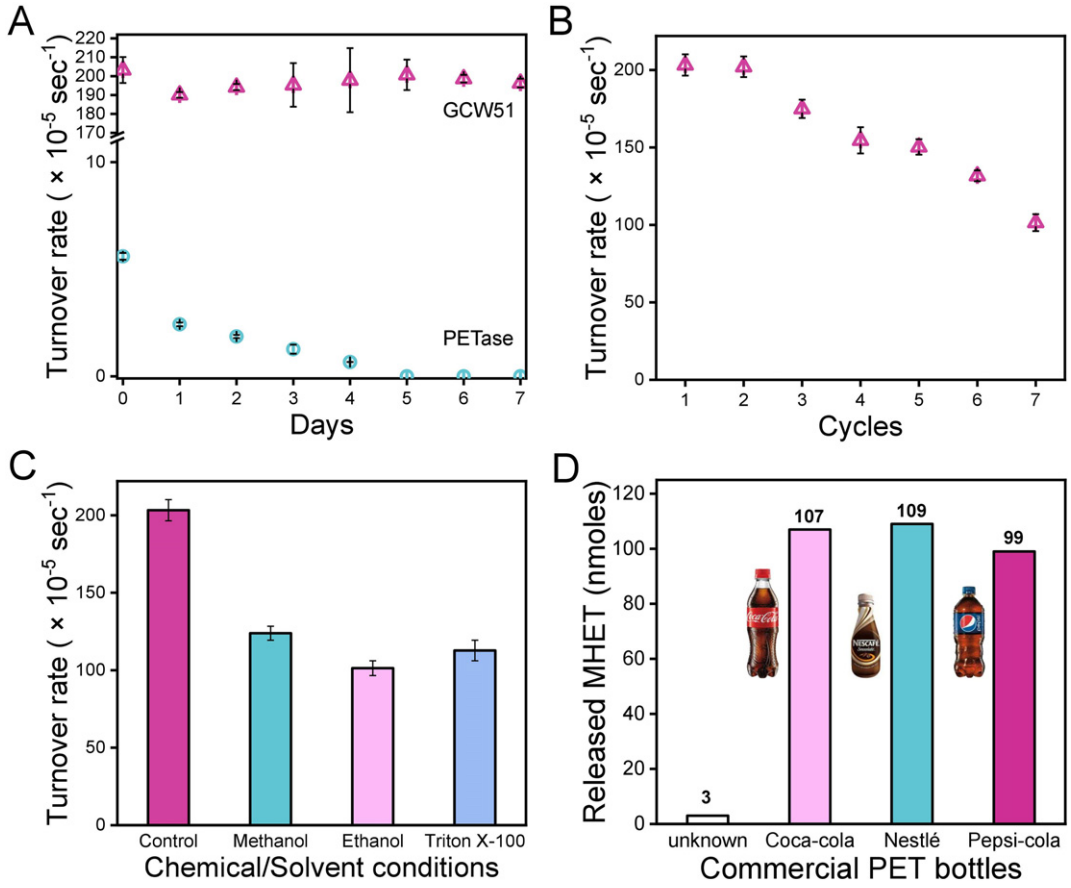

Fig. 5. (A) The thermostability of GS115/PETase-GCW51 and purified PETase. (B)Effect of recycling times and (C) Effect of Chemical/solvent conditions on PET film hydrolysis by *P. pastoris* GS115/PETase-GCW51. (D) Degradation of commercial PET bottles with the whole-cell biocatalyst. The first column of data was obtained from Yoshida S et al. (reference (Yoshida et al., 2016), and the second to fourth columns of data were measured by using the whole-cell biocatalyst).

recycling process is if the displayed PETase can retain its biological activity in this process. Therefore, the turnover rate of surface-displayed PETase was measured during each round of recycling (Fig. 5B). Overall, the turnover rate towards PET of surface-displayed PETase was maintained during the recycling process. For example, it was remained about 85% and 50% for three- and seven-round recycling respectively. The reusability of the whole-cell biocatalyst not only overcomes the problem that is native PETase is hard to recover from the reaction solution without the complicated and costly purification process but also makes it suitable for developing convenient and cost-effective biocatalyst process. Next, we investigated the stability of the whole-cell biocatalyst in some chemical/solvent conditions which may be used washing reagents to clean the used PET. The residual enzyme activity was measured after incubation of the whole-cell biocatalyst in normal reaction buffers containing 10% methanol, 10% ethanol and 0.1% Triton X-100 separately. As shown in Fig. 5C, the turnover rates remained around 50% at all the test conditions. This result reminded us to consider the effect of washing reagent on the degradation efficiency when we use the whole-cell biocatalyst system (Yuzbasheva et al., 2015). When the whole-cell biocatalyst is used in reality, its storage is also an important issue needs to be considered (Toscani et al., 2018). Fig. S7 shows the turnover rate of the whole-cell biocatalyst before and after freeze-dried. It was clear that the whole-cell biocatalyst retained almost total degradation ability after the dehydration process. The intracellular water is a disadvantage for the long-time storage of the yeast cell since bacterial contamination and macromolecular degradation occurs frequently in the watery environment. Freeze-dried yeast cells are obviously easy to store and transport than those of water containing cells. Finally, we applied the whole-cell biocatalyst to degrade commercial PET bottles. Fig. 5D shows our whole-cell biocatalyst can degrade different highly crystallized PET bottles. Compared to native PETase, surface-displayed PETase exhibited high degradation efficiency to the highly crystallized PET bottles. All the above results indicate the whole-cell biocatalyst we developed here has great potential to be applied in the large-scale degradation process of PET and finally contributes to the biological recycling of PET.

4. Conclusions

In this study, we developed, for the first time, a whole-cell biocatalyst based on surface displaying a novel PET-hydrolyzing enzyme PETase to degrade highly crystallized PET. We found that PETase could be functionally displayed on the surface of yeast (*P. pastoris*) cell. Anchor protein and induction time had great impacts on the enzymatic activity of displayed PETase. We also found that pH and thermal stability of PETase were increased after it was displayed on the surface of the yeast cell. Under optimized conditions, the enzymatic activity of the whole-cell biocatalyst towards the highly crystallized PET dramatically increased about 36-fold compared with the purified PETase. Moreover, the whole-cell biocatalyst could be reused for several times without significant losing activity. All those results indicated that PETase-displaying whole-cell biocatalyst affords a promising route for efficient biological degradation of PET. Based on our study, more whole-cell biocatalyst related to PETase may be developed in the future. For example, PETase mutants increasing the enzymatic activity can be surface displayed on the yeast cell to further enhance the performance of the whole-cell biocatalyst.

Declaration of competing interest

The authors declare that they have no known competing financial interests or personal relationships that could have appeared to influence the work reported in this paper.

Acknowledgment

Zefang Wang acknowledges the support of the National Natural Science Foundation of China (grant numbers 81601593 & 31970048).

Appendix A. Supplementary data

Supporting Information Available: method for western blot and immunofluorescence assay, treatment of PET film, HPLC analysis of degradation product of PET, standardization of cell number to protein concentration, optimization of protein concentration for PET hydrolysis reaction, effect of freeze-dried on PET film hydrolysis, and termination reaction. Strains, and plasmids used in this study (Table S1), primers used in this study (Table S2), sequence of PETase (Sequence S1), schematic of plasmids (Fig. S1), immunofluorescence staining of non-induced GS115/PETase-GCW21/51/61 (Fig. S2), the immunofluorescent staining of surface display cells (Fig. S3), the intensity of each western blot band and average fluorescence of tested cells with Image J software (Fig. S4), effect of protein concentration on PET hydrolysis (Fig. S5), standardization of cell number to protein concentration (Fig. S6), effect of freeze-dried on PET film hydrolysis (Fig. S7) and HPLC analysis of BHET before and after hydrolysis (Fig. S8), (PDF)Supplementary data to this article can be found online at https://doi.org/10.1016/j.scitotenv.2019.136138.

References

Annie, G.S., Dane, W.K., 2007. Yeast surface display for protein engineering and characterization. Curr. Opin. Struct. Biol. 17, 467–473. https://doi.org/10.1016/j.sbi.2007.08.012.

Austin, H.P., Allen, M.D., Donohoe, B.S., Rorrer, N.A., Kearns, F.L., Silveira, R.L., Pollard, B.C., Dominick, G., Duman, R., Omari, K.E., 2018. Characterization and engineering of a plastic-degrading aromatic polyesterase. Proc. Natl. Acad. Sci. 115, 4350–4357. https://doi.org/10.1073/pnas.1718804115.

Benavides, P.T., Dunn, J.B., Han, J., Biddy, M., Markham, J., 2018. Exploring comparative energy and environmental benefits of virgin, recycled, and bio-derived PET bottles. ACS Sustain. Chem. Eng. 6, 9725–9733. https://doi.org/10.1021/acssuschemeng.8b00750.

Bornscheuer, U.T., Huisman, G.W., Kazlauskas, R.J., Lutz, S., Moore, J.C., Robins, K., 2012. Engineering the third wave of biocatalysis. Nature 485, 185–194. https://doi.org/10.1038/nature11117.

Chen, Y., Stemple, B., Kumar, M., Wei, N., 2016. Cell surface display fungal laccase as a renewable biocatalyst for degradation of persistent micropollutants bisphenol a and sulfamethoxazole. Environmental Science & Technology 50, 8799–8808. https://doi.org/10.1021/acs.est.6b01641.

Cooney, C.L., 1983. Bioreactors: design and operation. Science 219, 728–733. https://doi.org/10.1126/science.219.4585.728.

Cressey, D., 2016. Bottles, bags, ropes and toothbrushes: the struggle to track ocean plastics. Nature 536, 263–265. https://doi.org/10.1038/536263a.

Doris, R., Antonio Orcal, Y., Sabine, Z., Jing, W., Susanne, N., Georg, S., Katrin, G., Ales, D., Gustav, O., Gruber, C.C., 2013. Fusion of binding domains to *Thermobifida cellulosilytica* cutinase to tune sorption characteristics and enhancing PET hydrolysis. Biomacromolecules 14, 1769–1776. https://doi.org/10.1021/bm400140u.

Fecker, T., Galaz-Davison, P., Engelberger, F., Narui, Y., Sotomayor, M., Parra, L.P., Ramírez-Sarmiento, C.A., 2018. Active site flexibility as a hallmark for efficient PET degradation by *I.sakaiensis* PETase. Biophys. J. 114, 1302–1312. https://doi.org/10.1016/j.bpj.2018.02.005.

Goyal, G., Tsai, S.L., Madan, B., Dasilva, N.A., Chen, W., 2011. Simultaneous cell growth and ethanol production from cellulose by an engineered yeast consortium displaying a functional mini-cellulosome. Microb. Cell Factories 10, 89. https://doi.org/10.1186/1475-2859-10-89.

Groß, C., Hamacher, K., Schmitz, K., Jager, S., 2017. Cleavage product accumulation decreases the activity of cutinase during PET hydrolysis. Journal of Chemical Information & Modeling 57, 243–255. https://doi.org/10.1021/acs.jcim.6b00556.

Guebitz, G.M., Cavaco-Paulo, A., 2008. Enzymes go big: surface hydrolysis and functionalisation of synthetic polymers. Trends Biotechnol. 26, 32–38. https://doi.org/10.1016/j.tibtech.2007.10.003.

Hahladakis, J.N., Velis, C.A., Weber, R., Iacovidou, E., Purnell, P., 2018. An overview of chemical additives present in plastics: migration, release, fate and environmental impact during their use, disposal and recycling. J. Hazard. Mater. 344, 179–199. https://doi.org/10.1016/j.jhazmat.2017.10.014.

Han, X., Liu, W., Huang, J.W., Ma, J., Zheng, Y., Ko, T.P., Xu, L., Cheng, Y.S., Chen, C.C., Guo, R.T., 2017. Structural insight into catalytic mechanism of PET hydrolase. Nat. Commun. 8, 2106. https://doi.org/10.1038/s41467-017-02255-z.

He, W., Jiang, B., Mu, W., Zhang, T., 2016. Production of d-allulose with d-psicose 3-epimerase expressed and displayed on the surface of *Bacillus subtilis* spores. J. Agric. Food Chem. 64, 7201–7207. https://doi.org/10.1021/acs.jafc.6b03347.

Global PET resin production capacity. https://www.plasticsinsight.com/global-pet-resin-production-capacity/.

Joo, S., Cho, I.J., Seo, H., Son, H.F., Sagong, H.Y., Shin, T.J., Choi, S.Y., Sang, Y.L., Kim, K.J., 2018. Structural insight into molecular mechanism of poly (ethylene terephthalate) degradation. Nat. Commun. 9, 382. https://doi.org/10.1038/s41467-018-02881-1.

Kawai, F., Kawabata, T., Oda, M., 2019. Current knowledge on enzymatic PET degradation and its possible application to waste stream management and other fields. Microbiology Biotechnology 103, 4253–4268. https://doi.org/10.1007/s00253-019-09717-y.

Lebreton, S., Zurzolo, C., Paladino, S., 2018. Organization of GPI-anchored proteins at the cell surface and its physiopathological relevance. Crit. Rev. Biochem. Mol. Biol. 53, 403–419. https://doi.org/10.1080/10409238.2018.1485627.

Lee, G.Y., Jung, J.-H., Seo, D.-H., Hansin, J., Ha, S.-J., Cha, J., Kim, Y.-S., Park, C.-S., 2011. Isomaltulose production via yeast surface display of sucrose isomerase from *Enterobacter* sp. FMB-1 on *Saccharomyces cerevisiae*. Bioresour. Technol. 102, 9179–9184. https://doi.org/10.1016/j.biortech.2011.06.081.

Lin, Y.H., Yang, M.H., 2007. Catalytic conversion of commingled polymer waste into chemicals and fuels over spent FCC commercial catalyst in a fluidised-bed reactor. Applied Catalysis B Environmental 69, 145–153. https://doi.org/10.1016/j.apcatb.2006.07.005.

Liu, X.Y., Chi, Z., Liu, G.L., Wang, F., Madzak, C., Chi, Z.M., 2010. Inulin hydrolysis and citric acid production from inulin using the surface-engineered *Yarrowia lipolytica* displaying inulinase. Metab. Eng. 12, 469–476. https://doi.org/10.1016/j.ymben.2010.04.004.

Liu, B., He, L., Wang, L., Li, T., Li, C., Liu, H., Luo, Y., Bao, R., 2018. Protein crystallography and site-direct mutagenesis analysis of the poly(ethylene terephthalate) hydrolase PETase from *Ideonella sakaiensis*. Chembiochem 19, 1471–1475. https://doi.org/10.1002/cbic.201800097.

Liu, M., Lu, X., Khan, A., Ling, Z., Wang, P., Tang, Y., Liu, P., Li, X., 2019. Reducing methylmercury accumulation in fish using *Escherichia coli* with surface-displayed methylmercury-binding peptides. J. Hazard. Mater. 367, 35–42. https://doi.org/10.1016/j.jhazmat.2018.12.058.

Mann, P.A., Mclellan, C.A., Koseoglu, S., Si, Q., Kuzmin, E., Flattery, A., Harris, G., Sher, X., Murgolo, N., Wang, H., 2015. Chemical genomics-based antifungal drug discovery: targeting glycosylphosphatidylinositol (GPI) precursor biosynthesis. ACS Infectious Diseases 1, 59–72. https://doi.org/10.1021/id5000212.

Paul, C., Bessette, P.H., David, K., Murr, M.M., Daugherty, P.S., Morse, D.E., 2005. Enzymatic synthesis of layered titanium phosphates at low temperature and neutral pH by cell-surface display of silicatein-alpha. J. Am. Chem. Soc. 127, 15749–15755. https://doi.org/10.1021/ja054307f.

Sardon, H., Dove, A.P., 2018. Plastics recycling with a difference. Science 360, 380–381. https://doi.org/10.1126/science.aat4997.

Shah, A.A., Hasan, F., Hameed, A., Ahmed, S., 2008. Biological degradation of plastics: a comprehensive review. Biotechnol. Adv. 26, 246–265. https://doi.org/10.1016/j.biotechadv.2007.12.005.

Shoda, S., Uyama, H., Kadokawa, J., Kimura, S., Kobayashi, S., 2016. Enzymes as green catalysts for precision macromolecular synthesis. Chem. Rev. 116, 2307–2413. https://doi.org/10.1021/acs.chemrev.5b00472.

Simon, F., Liron, A., Yearit, F., Amir, A., Lital, A., 2009. Surface display of redox enzymes in microbial fuel cells. J. Am. Chem. Soc. 131, 12052–12053. https://doi.org/10.1021/ja9042017.

Tanaka, T., Kondo, A., 2015. Cell surface engineering of industrial microorganisms for biorefining applications. Biotechnol. Adv. 33, 1403–1411. https://doi.org/10.1016/j.biotechadv.2015.06.002.

Taniguchi, I., Yoshida, S., Hiraga, K., Miyamoto, K., Kimura, Y., Oda, K., 2019. Biodegradation of PET: current status and application aspects. ACS Catal. 9, 4089–4105. https://doi.org/10.1021/acscatal.8b05171.

Toscani, A., Risi, C., Black, G.W., Brown, N.L., Castagnolo, D., 2018. Monoamine oxidase (MAO-N) whole cell biocatalyzed aromatization of 1,2,5,6-tetrahydropyridines into pyridines. ACS Catal. 8, 8781–8787. https://doi.org/10.1021/acscatal.8b02386.

Wu, C.H., Mulchandani, A., Chen, W., 2008. Versatile microbial surface-display for environmental remediation and biofuels production. Trends Microbiol. 16, 181–188. https://doi.org/10.1016/j.tim.2008.01.003.

Wu, L., Li, H., Tang, T., 2017. A novel yeast surface display method for large-scale screen inhibitors of sortase a. Bioengineering 4, 6. https://doi.org/10.3390/bioengineering4010006.

Wu, X., Fraser, K., Zha, J., Dordick, J.S., 2018. Flexible peptide linkers enhance the antimicrobial activity of surface-immobilized bacteriolytic enzymes. ACS Appl. Mater. Interfaces 10, 36746–36756. https://doi.org/10.1021/acsami.8b14411.

Xiaoying, C., Zaro, J.L., Wei-Chiang, S., 2013. Fusion protein linkers: property, design and functionality. Adv. Drug Deliv. Rev. 65, 1357–1369. https://doi.org/10.1016/j.addr.2012.09.039.

Xihong, H., Jiling, S., Fan, L., Hao, L., 2015. Yeast cell surface display of linoleic acid isomerase from *Propionibacterium acnes* and its application for the production of trans-10, cis-12 conjugated linoleic acid. Biotechnol. Appl. Biochem. 62, 1–8. https://doi.org/10.1002/bab.1249.

Yang, C.E., Chu, I.M., Wei, Y.H., Tsai, S.L., 2017. Surface display of synthetic phytochelatins on *Saccharomyces cerevisiae* for enhanced ethanol production in heavy metal-contaminated substrates. Bioresour. Technol. 245, 1455–1460. https://doi.org/10.1016/j.biortech.2017.05.127.

Yin, K., Lv, M., Wang, Q., Wu, Y., Liao, C., Zhang, W., Chen, L., 2016. Simultaneous bioremediation and biodetection of mercury ion through surface display of carboxylesterase E2 from *Pseudomonas aeruginosa* PA1. Water Res. 103, 383–390. https://doi.org/10.1016/j.watres.2016.07.053.

Yoshida, S., Hiraga, K., Takehana, T., Taniguchi, I., Yamaji, H., Maeda, Y., Toyohara, K., Miyamoto, K., Kimura, Y., Oda, K., 2016. A bacterium that degrades and assimilates poly(ethylene terephthalate). Science 351, 1196–1199. https://doi.org/10.1126/science.aad6359.

Yuzbasheva, E.Y., Yuzbashev, T.V., Perkovskaya, N.I., Mostova, E.B., Vybornaya, T.V., Sukhozhenko, A.V., Toropygin, I.Y., Sineoky, S.P., 2015. Cell surface display of *Yarrowia lipolytica* lipase Lip2p using the cell wall protein YlPir1p, its characterization, and application as a whole-cell biocatalyst. Appl. Biochem. Biotechnol. 175, 3888–3900. https://doi.org/10.1007/s12010-015-1557-7.

Zhang, S., Jiang, Z., Shi, J., Wang, X., Han, P., Qian, W., 2016. An efficient, recyclable and stable immobilized biocatalyst based on bioinspired microcapsules-in-hydrogel scaffolds. ACS Appl. Mater. Interfaces 8, 25152–25161. https://doi.org/10.1021/acsami.6b09483.

Zhang, X., Fevre, M., Jones, G.O., Waymouth, R.M., 2017. Catalysis as an enabling science for sustainable polymers. Chem. Rev. 118, 839–885. https://doi.org/10.1021/acs.chemrev.7b00329.

Zhu, B., Wei, N., 2019. Biocatalytic degradation of parabens mediated by cell surface displayed cutinase. Environmental Science & Technology 53, 354–364. https://doi.org/10.1021/acs.est.8b05275.